Few-Body Syst (2018) 59:82
https://doi.org/10.1007/s00601-018-1405-8

Daniel S. Carman

CLAS N^* Excitation Results from Pion and Kaon Electroproduction

Received: 30 December 2017 / Accepted: 11 May 2018

Abstract The study of the structure of excited nucleon N^* states using the electroproduction of exclusive reactions is important for exploring the non-perturbative strong interaction. The electrocoupling amplitudes of N^* states for masses below $W = 1.8$ GeV have been determined from analyses of CLAS πN, ηN, and $\pi\pi N$ data at four momentum transfers Q^2 up to 5 GeV^2. These studies have made it apparent that consistency of the results from independent analyses of multiple exclusive channels with different couplings and non-resonant backgrounds but the same N^* electroexcitation amplitudes, is necessary to have confidence in the results. For the hadronic couplings, many high-lying N^* states preferentially decay through the $\pi\pi N$ channel instead of the πN channel. Therefore, data from the KY channels already measured with CLAS will be crucial to provide an independent analysis to compare the extracted electrocouplings for the high-lying N^* states against those determined from the πN and $\pi\pi N$ channels. These comparisons await the development of suitable reaction models. Starting in 2018, a program to study the structure of N^* states in various exclusive electroproduction channels using the new CLAS12 spectrometer will get underway. These studies will probe the structure of these states for masses W up to 3 GeV and Q^2 up to 12 GeV^2, thus providing a means to access N^* structure information spanning a broad regime encompassing both low and high energy degrees of freedom.

Keywords Electromagnetic interactions · Form factors · Nucleon structure · Excited nucleon states

1 Introduction

Intensive studies of the spectrum and structure of excited nucleon (N^*) states have played a crucial role in the development of our understanding of the strong interaction within the light quark sector. As a result of intense experimental and theoretical effort over the past 40 years, it is now apparent that the structure of N^* states is much more complex than what can be described in terms of models based on constituent quarks alone. At the typical energy and distance scales found within the N^* states, the quark-gluon coupling is large. Therefore, we are confronted with the fact that quark-gluon confinement, hadron mass generation, and the dynamics that give rise to the N^* spectrum, cannot be understood within the framework of perturbative Quantum Chromodynamics (QCD). The need to understand QCD in this non-perturbative domain is a fundamental issue in nuclear physics, which the study of N^* structure can help to address. Such studies, in fact, represent a necessary step toward understanding how QCD in the regime of large quark-gluon couplings generates mass and how systems

This article belongs to the Topical Collection "NSTAR 2017 - The International Workshop on the Physics of Excited Nucleons".

Daniel S. Carman: for the CLAS Collaboration.

Daniel S. Carman (✉)
Jefferson Laboratory, 12000 Jefferson Ave., Newport News, VA 23606, USA
E-mail: carman@jlab.org

Published online: 24 May 2018

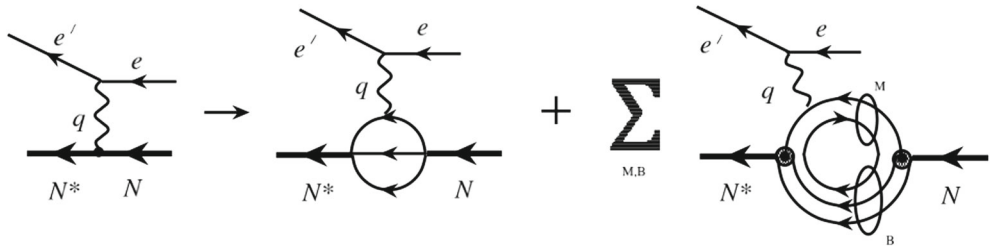

Fig. 1 Schematic representation of the $\gamma^* N \rightarrow N^*$ electroproduction process. **a** The fully dressed $\gamma_v N N^*$ electrocoupling that determines the N^* contribution to the resonant part of the meson electroproduction amplitude. **b** The contribution of the three-quark core. **c** The contribution from the meson–baryon cloud, where the sum is over all intermediate meson and baryon states. This figure was taken from Ref. [7]

of confined quarks and gluons, i.e. mesons and baryons, are formed. These questions are among the most challenging open problems within the Standard Model of fundamental particles and interactions [1].

Studies of low-lying nucleon excited states using electromagnetic probes at four momentum transfers $Q^2 < 5$ GeV^2 have revealed that the structure of N^* states is a complex interplay between the internal core of three dressed quarks and an external field of quark-antiquark pairs referred to as the meson–baryon (M–B) cloud. N^* states of different quantum numbers have significantly different relative contributions from these two components, demonstrating distinctly different manifestations of the non-perturbative strong interaction in their generation. The relative contribution of the quark core increases with Q^2 in a gradual transition to a dominance of quark degrees of freedom for $Q^2 > 5$ GeV^2. This kinematics area still remains almost unexplored in exclusive reactions. Studies of the Q^2 evolution of N^* structure from low to high Q^2 offer access to the strong interaction between dressed quarks in the non-perturbative regime that is responsible for N^* formation.

Electroproduction reactions of the form $\gamma^* N \rightarrow N^* \rightarrow M + B$ provide a tool to probe the inner structure of the contributing N^* resonances through the extraction of the amplitudes that describe the transition between the virtual photon–nucleon initial state and the intermediate excited N^* state. These $\gamma_v N N^*$ electrocoupling amplitudes are directly related to the structure of their associated N^* states and can be represented by the so-called transition helicity amplitudes $A_{1/2}(Q^2)$, $A_{3/2}(Q^2)$, and $S_{1/2}(Q^2)$. $A_{1/2}$ and $A_{3/2}$ describe the N^* resonance electroexcitation for the different configurations of helicity for a transverse photon and a nucleon with helicity parallel or anti-parallel to the photon. $S_{1/2}$ describes the N^* resonance electroexcitation by longitudinal photons of zero helicity [2]. The Q^2 evolution of these electrocoupling amplitudes provides fundamental information on the relevant degrees of freedom that describe the structure of the nucleon as a function of distance scale. These fundamental quantities are now subject to computations starting from theoretical approaches based on the QCD Lagrangian.

Detailed comparisons of the theoretical predictions for these amplitudes against the experimental measurements form the basis of gauging our progress toward understanding of non-perturbative QCD. The measurement of the electrocouplings is essential in order to access the dynamical momentum-dependent mass and structure of dressed quarks in the non-perturbative domain where the quark-gluon coupling is large [3], through mapping of the dressed quark mass function [4] and extraction of the quark distribution amplitudes for N^* states of different quantum numbers [5]. This is critical in exploring the nature of quark-gluon confinement and dynamical chiral symmetry breaking (DCSB) in baryons.

Figure 1 shows a schematic representation of the $\gamma^* N \rightarrow N^*$ electroproduction process. In Fig. 1b the virtual photon interacts directly with the constituent quark, an interaction that is sensitive to the quark current and depends on the quark-mass function. However, the full meson electroproduction amplitude in Fig. 1a requires contributions to the $\gamma_v N N^*$ vertex from both non-resonant meson electroproduction and the hadronic scattering amplitudes as shown in Fig. 1c. These contributions incorporate all possible intermediate meson–baryon states and meson–baryon scattering processes that eventually result in N^* formation in the intermediate state of the reaction. These two contributions can be separated from each another using, for example, a coupled-channel reaction model [6].

Current theoretical approaches to understand N^* structure fall into two broad categories. In the first are those that enable direct connection to the QCD Lagrangian, such as Lattice QCD (LQCD) and Dyson-Schwinger equation (DSE) calculations. In the second are those that use models inspired by or derived from our knowledge of QCD, such as quark-hadron duality, light-front holographic QCD (AdS/QCD), light-cone sum rules (LCSR),

and Constituent Quark Models (CQMs). See Ref. [7] for an overview of these different approaches. It is important to realize that even those approaches that attempt to solve QCD directly can only do so approximately. As such, it is imperative that whenever possible, the results of these intensive and challenging calculations be compared directly to the data on resonance electrocouplings from electroproduction experiments over a broad range of Q^2 for N^* states with different quantum numbers.

The complete N^* spectrum is predicted by CQMs to consist of a sizable number of states that extend from the $N(1440)\frac{1}{2}^+$ Roper resonance to states with masses up to 3 GeV and beyond [8,9]. Our current knowledge of the spectrum of N^* and Δ^* states is mainly based on a large body of $\pi - N$ elastic scattering data. However, if a resonance couples weakly to the πN channel, or if its decay width is sufficiently broad, or if the state has significant overlap with other nearby resonances, it could have been missed in the extraction analysis. Reasons such as these (among others) could explain the long-standing missing resonance puzzle. This puzzle refers to the disparity between the large number of s-channel baryon resonance states predicted by the CQM models and the relatively few determined from the available scattering data. In this regard, it is important to make clear that the large number of N^* states and the specifics as to their masses, orderings, and quantum numbers is fully supported by recent Lattice QCD predictions [10]. For completeness it is important to mention that there are theoretical models that predict a significantly reduced spectrum of excited nucleon states compared to CQM and LQCD predictions. These models include those based on a reduced dimensionality in terms of the number of degrees of freedom and include diquark models among others.

The missing resonance puzzle is one of the primary aspects of the N^* studies in Hall B at Jefferson Laboratory (JLab). This effort focuses specifically on studies of the nucleon excitation spectrum via both photo- and electroproduction of s-channel resonance states decaying to a variety of different final states. The output of this program has provided a wealth of new precision information on both the spectrum and structure of the N^* states.

2 CLAS N^* Program

Studies of the structure of the excited nucleon states, the so-called N^* program, is one of the cornerstones of the physics program in Hall B at JLab. The large acceptance spectrometer CLAS [11], which began data taking in 1997 and was decommissioned in 2012, was designed to measure photo- and electroproduction cross sections and polarization observables for beam energies up to 6 GeV over a broad kinematic range for a host of different exclusive reaction channels.

The photoproduction data sets from CLAS and elsewhere have been used extensively to constrain coupled-channel fits and advanced single-channel models. However, data at $Q^2 = 0$ allows for the identification of N^* states and the determination of their quantum numbers, but provide very little information about the structure of these states. It is the Q^2 dependence of the $\gamma_v NN^*$ electrocouplings that unravel and reveal these details. In addition, electrocoupling data are promising for N^* studies as the ratio of the resonant to non-resonant amplitudes increases with increasing Q^2 as seen in recent studies of CLAS $\pi\pi p$ data [12].

The goal of the N^* program with CLAS is to study the spectrum of N^* states and their associated structure over a broad range of distance scales through studies of the Q^2 dependence of the $\gamma_v NN^*$ electrocouplings. An important constraint on the studies of electroproduction data is that the fit parameters for the N^* states must be described by Q^2-independent resonance masses and hadronic decay widths. The goal to extract the N^* resonance electrocouplings from the data is realized through two distinct phases. The first phase consists of the measurements of the cross sections and polarization observables in as fine a binning in the relevant kinematic variables Q^2, W, $d\tau_{hadrons}$ (where $d\tau_{hadrons}$ represents the phase space of the final state hadrons) as the data support. The second phase consists of employing advanced reaction models that completely describe the data over its full phase space in order to then extract the electrocoupling amplitudes for the dominant contributing N^* states in each different reaction channel. Consistent determination of N^* properties from different exclusive channels with different couplings and non-resonant backgrounds offers model-independent support for the findings.

2.1 Non-strange Final States

The CLAS electroproduction program for studies of the spectrum and structure of excited nucleon states has focused extensively on the measurement of non-strange exclusive final states over a range of invariant energy W

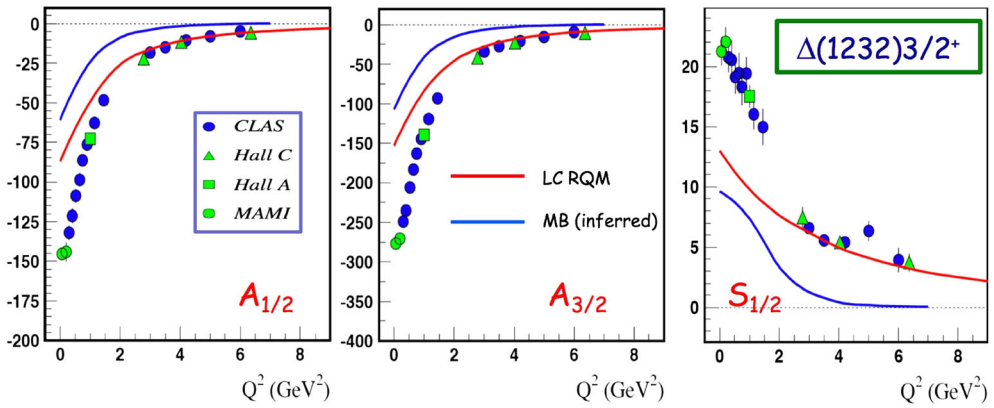

Fig. 2 The $A_{1/2}$, $A_{3/2}$, and $S_{1/2}$ electrocoupling amplitudes (in units of 10^{-3} GeV$^{-1/2}$) versus Q^2 (GeV^2) for the $\Delta(1232)\frac{3}{2}^+$ from analyses of πN data from CLAS (blue circles) [14], JLab Hall A (green squares) [21], JLab Hall C (green triangles) [22,23], and MAMI (green circles) [24]. The calculations are from a non-relativistic light-front quark model with a running quark mass (red line) [25]. The inferred magnitude of the meson–baryon cloud contributions is shown by the blue line as the difference between the data and the quark model calculation

up to 3 GeV and Q^2 from the photon point up to 6 GeV^2. Cross sections and various polarization observables, including measurements with polarized beam and targets, are available for the reactions: $ep \rightarrow e'p'\pi^0$, $ep \rightarrow e'n\pi^+$, $ep \rightarrow e'p'\pi^+\pi^-$, $en \rightarrow e'p'\pi^-$, $ep \rightarrow e'p'\omega$, $ep \rightarrow e'p'\rho^0$, $ep \rightarrow e'p'\phi$, and $ep \rightarrow e'p'\eta$. The full datasets are available within the CLAS physics database [13].

Electrocoupling amplitudes for most N^* states below 1.8 GeV have been extracted for the first time from analysis of CLAS ep data in the exclusive π^+n and π^0p channels for Q^2 up to 5 GeV^2, in ηp for Q^2 up to 4 GeV^2, and for $\pi^+\pi^-p$ for Q^2 up to 5 GeV^2. These data include unpolarized differential cross sections, longitudinally polarized beam asymmetries, and longitudinal target and beam-target spin asymmetries. Resonance extractions from cross section and polarization data represent a complex exercise and involve a level of model and fit uncertainty. Therefore it is highly desirable that the resonance transitions are determined from at least two different final states.

The available πN data from CLAS and elsewhere have been analyzed within the framework of two conceptually different approaches based on a unitary isobar model (UIM) and a dispersion relation (DR) approach [14,15]. The UIM describes the N^* electroproduction amplitudes as a superposition of N^* electroexcitations in the s-channel, non-resonant Born terms, and ρ and ω t-channel contributions. In the DR approach, dispersion relations are employed that relate the real to the imaginary parts of the invariant amplitudes that describe the N^* electroproduction. Both approaches provide a good description of the πN data over the range of the available measurements. The $\pi^+\pi^-p$ electroproduction data from CLAS [12,16,17] have been fit within the JM reaction model [18,19] with the goal of extracting resonance electrocouplings, as well as the $\pi\Delta$ and ρp hadronic decay widths. This model incorporates all relevant reaction mechanisms in the $\pi^+\pi^-p$ final state [20].

Figure 2 shows the $A_{1/2}$, $A_{3/2}$, and $S_{1/2}$ electrocouplings for the $\Delta(1232)\frac{3}{2}^+$ from analysis of π^0p data from CLAS [14], JLab Halls A and C [21–23], and MAMI [24]. This figure shows model predictions from the Light Cone Relativistic Quark Model (red curves) [25] and an estimate of the meson cloud contributions (blue curves) from the difference between the data and the quark model predictions. Figure 3 shows representative CLAS data for the $A_{1/2}$ electrocouplings for the N^* states $N(1440)\frac{1}{2}^+$, $N(1520)\frac{3}{2}^-$, and $N(1675)\frac{5}{2}^-$ from independent analyses of πN and $\pi\pi N$ data from CLAS [7,18,19,26]. Studies of the electrocouplings for N^* states of different quantum numbers at lower Q^2 have revealed a very different interplay between the inner quark core and the meson–baryon cloud as a function of Q^2. In fact, structure studies of the low-lying N^* states have made significant progress in recent years due to the agreement of results from independent analyses of the CLAS πN and $\pi\pi N$ final states [18]. The good agreement of the extracted electrocouplings from both the πN and $\pi\pi N$ final states is non-trivial in that these channels have very different mechanisms for the non-resonant backgrounds. The agreement thus provides compelling evidence for the reliability of the results.

The size of the meson–baryon dressing amplitudes are maximal for $Q^2 < 1$ GeV^2 (see Figs. 2 and 3). For increasing Q^2, there is a gradual transition to the domain where the quark degrees of freedom begin to

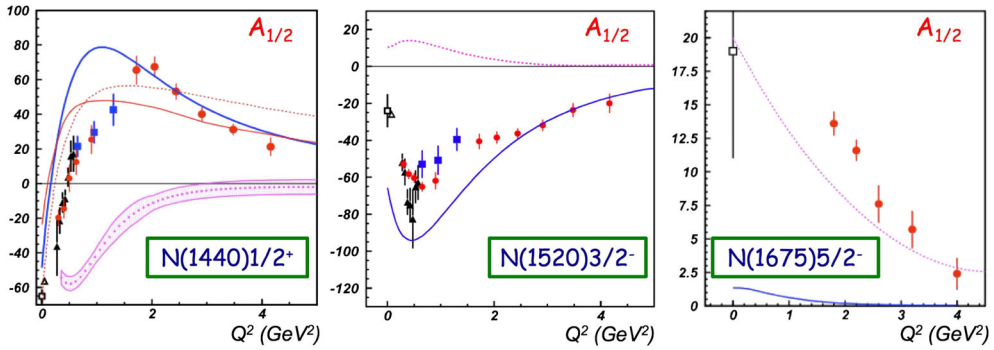

Fig. 3 The $A_{1/2}$ electrocoupling amplitudes (in units of 10^{-3} GeV$^{-1/2}$) versus Q^2 (GeV^2) for the N^* states $N(1440)\frac{1}{2}^+$ (left), $N(1520)\frac{3}{2}^-$ (middle), and $N(1675)\frac{5}{2}^-$ (right) from analyses of the CLAS πN (circles) and $\pi\pi N$ (triangles, squares) data [7,18,19,26]. (Left) Calculation from a non-relativistic light-front quark model with a running quark mass (red line) [25] and calculation of the quark core from the DSE approach (blue line) [3]. (Middle/Right) Calculations from the hypercentral constituent quark model (blue lines) [27]. An estimate of the meson–baryon cloud contributions is shown by the magenta line (or band) on each plot [28]

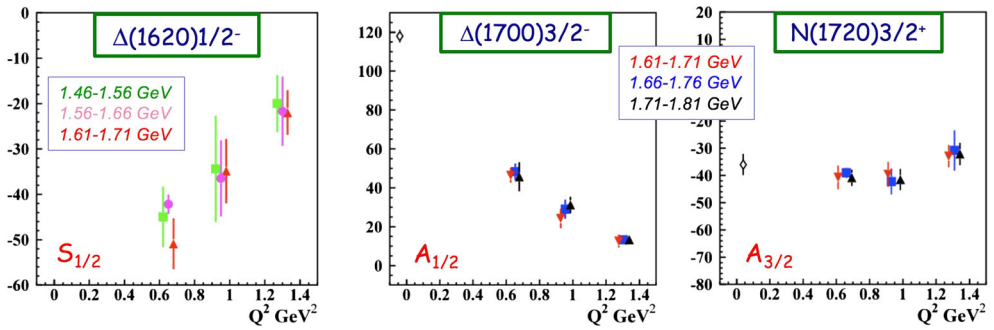

Fig. 4 CLAS results for the N^* electrocoupling amplitudes (in units of 10^{-3} GeV$^{-1/2}$) from analysis of the exclusive $\pi^+\pi^- p$ final state as a function of Q^2 (GeV^2). (Left) $S_{1/2}$ of the $\Delta(1620)\frac{1}{2}^-$ [19], (middle) preliminary extraction of $A_{1/2}$ for the $\Delta(1700)\frac{3}{2}^-$ [26], and (right) preliminary extraction of $A_{3/2}$ for the $N(1720)\frac{3}{2}^+$ [26]. Each electrocoupling amplitude was extracted in independent fits in different bins of W across the resonance peak width as shown for each Q^2 bin (points in each Q^2 bin offset for clarity)

dominate, as seen by the improved description of the N^* electrocouplings obtained within the DSE approach (see Fig. 3), which accounts only for the quark core contributions. The quark core contribution can also be predicted within the hypercentral CQM [27]. For $Q^2 > 5$ GeV^2, the quark degrees of freedom are expected to fully dominate the N^* states [7]. Therefore, in the $\gamma_v NN^*$ electrocoupling studies for $Q^2 > 5$ GeV^2 that are part of the planned CLAS12 N^* program (see Sect. 3), the quark degrees of freedom will be probed more directly with only small contributions from the meson–baryon cloud.

Studies of the electrocouplings for the $\Delta(1232)\frac{3}{2}^+$ and $N(1440)\frac{1}{2}^+$ states versus Q^2 within the DSE approach [3] have explicitly demonstrated sensitivity to the momentum-dependent evolution of the dressed quark mass function. This mass function can now be effectively "measured" as it influences and determines the electrocoupling amplitudes. This fundamental ingredient of QCD provides direct insight into the emergence of $> 98\%$ of the mass of the hadron.

Analysis of CLAS data for the $\pi\pi N$ channel has provided the only detailed structural information available regarding higher-lying nucleon excited states, e.g. $\Delta(1620)\frac{1}{2}^-$, $N(1650)\frac{1}{2}^-$, $N(1680)\frac{5}{2}^+$, $\Delta(1700)\frac{3}{2}^-$, and $N(1720)\frac{3}{2}^+$. This is due to the fact that most N^* states with masses above 1.6 GeV decay preferentially through the $\pi\pi N$ channel instead of the πN channel. Figure 4 shows a representative set of illustrative examples for $S_{1/2}$ for the $\Delta(1620)\frac{1}{2}^-$ [19], $A_{1/2}$ for the $\Delta(1700)\frac{3}{2}^-$, and $A_{3/2}$ for the $N(1720)\frac{3}{2}^+$ [26]. Here the analysis for each N^* state was carried out independently in different bins of W across the width of the resonance for Q^2 up to 1.5 GeV^2 with very good correspondence within each Q^2 bin. An up-to-date list of the N^* photo- and electrocouplings extracted from the experimental data from CLAS and elsewhere are available in Ref. [29].

Table 1 The states and associated kinematic ranges for CLAS data from which the $\gamma_v NN^*$ electrocouplings have been extracted. The first column lists the reaction channel and the last column provides the Q^2 range for which the extractions were made. See Ref. [29] for the electrocoupling values and the associated data references

Reaction channel	N^*, Δ^* states	Q^2 ranges (GeV^2)
$\pi^0 p$, $\pi^+ n$	$\Delta(1232)\frac{3}{2}^+$	0.16–6.0
	$N(1440)\frac{1}{2}^+$, $N(1520)\frac{3}{2}^-$, $N(1535)\frac{1}{2}^-$	0.30–4.16
$\pi^+ n$	$N(1675)\frac{5}{2}^-$, $N(1680)\frac{5}{2}^+$, $N(1710)\frac{1}{2}^+$	1.6–4.5
ηp	$N(1535)\frac{1}{2}^-$	0.2–0.9
$\pi^+\pi^- p$	$N(1440)\frac{1}{2}^+$, $N(1520)\frac{3}{2}^-$	0.25–1.5
	$\Delta(1620)\frac{1}{2}^-$, $N(1650)\frac{1}{2}^-$, $N(1680)\frac{5}{2}^+$,	0.5–1.5
	$\Delta(1700)\frac{3}{2}^-$, $N(1720)\frac{3}{2}^+$, $N'(1720)\frac{3}{2}^+$	

This webpage also includes all of the references to the data and to the determination of the amplitudes. The available electrocoupling amplitudes from analysis of CLAS data are summarized in Table 1, listing the reaction channel studied, the different N^* and Δ^* states for which the $\gamma_v NN^*$ electrocouplings are available, and the Q^2 range of the experimental data for which the extractions were made.

2.2 Strange Final States

With a goal to have an independent determination of the electrocouplings for each N^* state from multiple exclusive reaction channels, a natural avenue to investigate for the higher-lying N^* states is the strangeness channels $K^+\Lambda$ and $K^+\Sigma^0$. In fact, data from the KY channels are critical to provide an independent extraction of the electrocoupling amplitudes for the higher-lying N^* states and represent a central part of the N^* program planned with CLAS12 [30] (see Sect. 3). For most N^* states with coupling to KY, the πN coupling is larger than the KY coupling. In other words, $g_{\pi NN} > g_{KYN}$. However, there are states for which the KY coupling is predicted to be of the same magnitude (or even larger) than the πN coupling. In addition, in cases where the πN coupling is weak, it may be that pulling out N^* states from πN elastic scattering experimental data could be quite difficult. Therefore, the study of KY final states should be viewed as complementary to the study of πN final states. It is also important to make clear that due to the fact that $m_K + m_Y > m_\pi + m_N$, the KY decays kinematically favor a two-body decay mode for resonances with masses near 2 GeV. This amounts to a significant experimental advantage for the study of $N^* \rightarrow KY$ decays as two-body decay modes are easier to interpret than extracting N^* spectrum and structure information from the reconstruction of a series of sequential non-strange decays. In comparison to the πN, $\pi\pi N$, and other prominent non-strange channels, the backgrounds for the KY channels are quantitatively and qualitatively different as are the resonant to non-resonant amplitude contributions. In such a case, the systematics of the extracted electrocoupling amplitudes would be wholly different. Consistency of the extracted amplitudes from the independent analysis of the non-strange and strange final states would then serve to give confidence in the results.

Another significant benefit of studying N^* decays to the KY strangeness channels is that the recoil polarizations are readily accessible due to the self-analyzing nature of the hyperon weak decays. Analysis of hyperon recoil and beam-recoil observables for $K^+\Lambda$ and $K^+\Sigma^0$ final states has been completed as part of the CLAS electroproduction analysis (see below). The importance of hyperon polarization data has been of key importance in the recent advances that have been made in understanding the N^* spectrum through coupled-channel fits as discussed below. Studies of the N^* spectrum extended to include the available CLAS electroproduction data in different bins of Q^2 should provide for important cross-checks to the results gleaned from the photoproduction data.

With regard to the KY channels, measurements of both the $K^+\Lambda$ and $K^+\Sigma^0$ channels are essential to unravel the spectrum and structure of N^* and Δ^* states. Although these two ground-state hyperons have the same valence quark structure (uds), they differ in isospin, such that intermediate N^* resonances can decay strongly to $K^+\Lambda$ final states, but intermediate Δ^* states cannot. Because $K^+\Sigma^0$ final states can have contributions from both N^* and Δ^* states, the hyperon final state selection constitutes an isospin filter.

Within the PDG listings for the past several decades, only four N^* states were listed with known coupling to $K^+\Lambda$, $N(1650)\frac{1}{2}^-$, $N(1710)\frac{1}{2}^+$, $N(1720)\frac{3}{2}^+$, and $N(1900)\frac{3}{2}^+$, and no states were listed with coupling

Table 2 Listing of N^* states in the review of particle properties [35] with much improved evidence as observed in the Bonn-Gatchina partial wave analysis based on studies of the CLAS KY photoproduction data [36,37]. The last three columns show the importance of the $K^+\Lambda$, $K^+\Sigma^0$, and γN couplings in the observation of these states. This table was taken from Ref. [39]

	RPP pre-2012	RPP 2014/2016	$K^+\Lambda$	$K^+\Sigma^0$	γN
$N(1710)\frac{1}{2}^+$	***	****	****	**	****
$N(1880)\frac{1}{2}^+$		**	**		**
$N(1895)\frac{1}{2}^-$		**	**	*	**
$N(1900)\frac{3}{2}^+$	**	***	***	**	***
$N(1875)\frac{3}{2}^-$		***	***	**	***
$N(2150)\frac{3}{2}^-$		**	**		**
$N(2000)\frac{5}{2}^+$	*	**	**	*	**
$N(2060)\frac{5}{2}^-$		**		**	**

strength to $K^+\Sigma^0$ [31]. Furthermore, only a single Δ^* state, $\Delta(1920)\frac{3}{2}^+$, was listed with coupling strength to $K^+\Sigma^0$. The uncertainties on the determined branching fractions for the few states listed were comparable with the measured values. Several studies in recent years have shown that these listed N^* and Δ^* states with coupling to KY are completely insufficient toward being able to reproduce the available experiment data for $W < 2$ GeV [32,33]. These analyses have even indicated that the coupling of $N(1710)\frac{1}{2}^+$ to $K^+\Lambda$ is much weaker than indicated by these older PDG values.

A recent development that has significantly advanced the studies of the spectrum of N^* states was provided by the Bonn-Gatchina coupled channel partial wave analysis of the hadronic πN and photoproduced γp channels [34]. This work provided a wholly updated listing of pole parameters and branching fractions for all N^* and Δ^* states up to ~2 GeV. The listed uncertainties are provided from this work at the few percent level.

The relevance of the strangeness channels $K^+\Lambda$ and $K^+\Sigma^0$ has been made clear in the work by the Bonn-Gatchina group. Their analysis has provided evidence for a set of eight N^* states that are either newly discovered or for which evidence of their existence is much improved (see Table 2). These states are included in the recent edition of the Review of Particle Properties [35]. These findings have critically relied upon the hyperon photoproduction data from CLAS [36,37]. In total, in the range below $W \sim 2.2$ GeV, the present PDG listings provide evidence of coupling for 12 N^* states to $K\Lambda$ and 11 N^* states with coupling to $K\Sigma$. In addition, 5 Δ^* states are listing with coupling to $K\Sigma$ [38].

The CLAS program has yielded by far the most extensive and precise measurements of KY electroproduction data ever measured across the nucleon resonance region. These measurements have included the separated structure functions σ_T, σ_L, $\sigma_U = \sigma_T + \epsilon\sigma_L$, σ_{LT}, σ_{TT}, and $\sigma_{LT'}$ for $K^+\Lambda$ and $K^+\Sigma^0$ [40–43], recoil polarization for $K^+\Lambda$ [44], and beam-recoil transferred polarization for $K^+\Lambda$ and $K^+\Sigma^0$ [45,46]. These measurements span Q^2 from 0.5 to 4.5 GeV^2, W from 1.6 to 3.0 GeV, and the full center-of-mass angular range of the K^+ [30]. The KY final states, due to the creation of an $s\bar{s}$ quark pair in the intermediate state, are naturally sensitive to coupling to higher-lying s-channel resonance states at $W > 1.6$ GeV, a region where our knowledge of the N^* spectrum is the most limited.

Shown in Figs. 5 and 6 is a small sample of the available data from CLAS in the form of the $K^+\Lambda$ and $K^+\Sigma^0$ structure functions $\sigma_U, \sigma_{LT}, \sigma_{TT}$, and $\sigma_{LT'}$ [43], illustrating its broad kinematic coverage and statistical precision. Figure 7 shows the Λ induced polarization from CLAS data for the reaction $ep \rightarrow e'K^+\Lambda$ at an average Q^2 of 1.9 GeV^2 for different angular ranges for $\cos\theta_K^{cm}$ taken with a 5.5 GeV beam [44]. The full CLAS KY electroproduction datasets are included in the CLAS physics database [13].

At the present time the N^* and Δ^* spectrum and structure information available from data on decays to the KY strangeness final states is at a significantly lower level compared to the information available from studies of the non-strange final states. This is not due to a dearth of available data from measurements of the electroproduction of KY, especially given the significant data already available from measurements with CLAS (discussed below). The main reason is the lack of available reaction models that are sufficiently accurate to account for the data.

Figures 5, 6, and 7 include two of the more advanced single channel reaction models for the electromagnetic production of KY final states. The MX model is the isobar model from Maxwell [47] (red curves), and the RPR-2007 [48] and RPR-2011 [49] models are from the Ghent Regge plus Resonance (RPR) framework

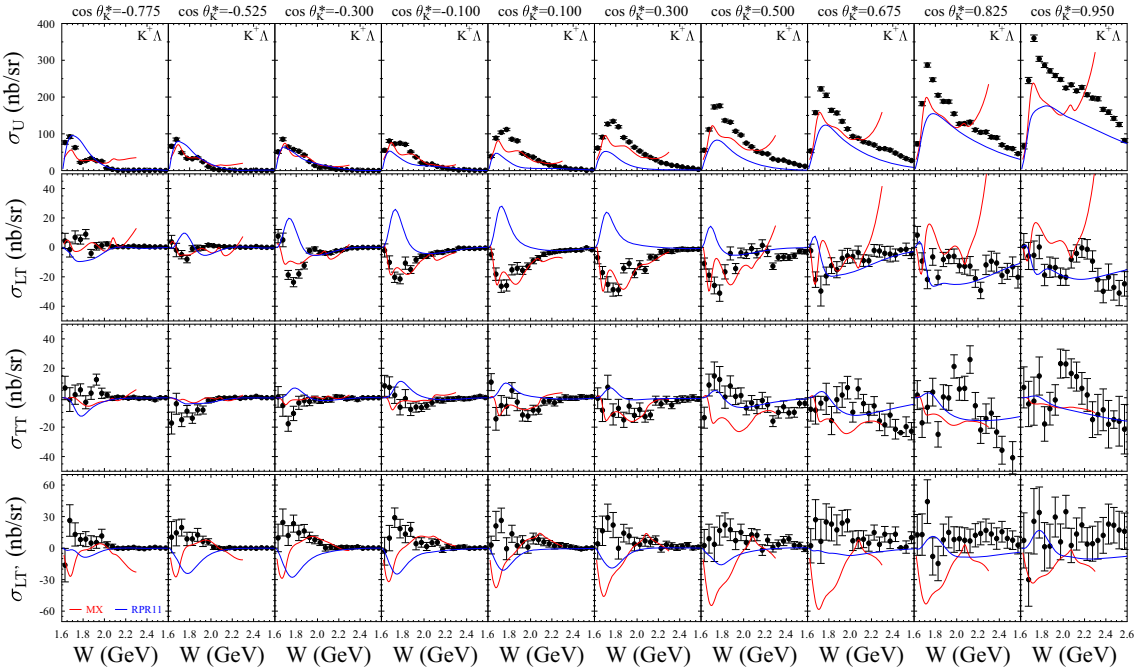

Fig. 5 Structure functions $\sigma_U = \sigma_T + \epsilon\sigma_L$, σ_{LT}, σ_{TT}, and $\sigma_{LT'}$ (nb/sr) from CLAS data for $K^+\Lambda$ production versus W (GeV) for E_{beam}=5.5 GeV for Q^2=1.80 GeV^2 and $\cos\theta^*_K$ values as shown [43]. The error bars represent the statistical uncertainties only. The red curves are from the hadrodynamic KY model of Maxwell [47] and the blue curves are from the hybrid RPR-2011 KY model from Ghent [49]

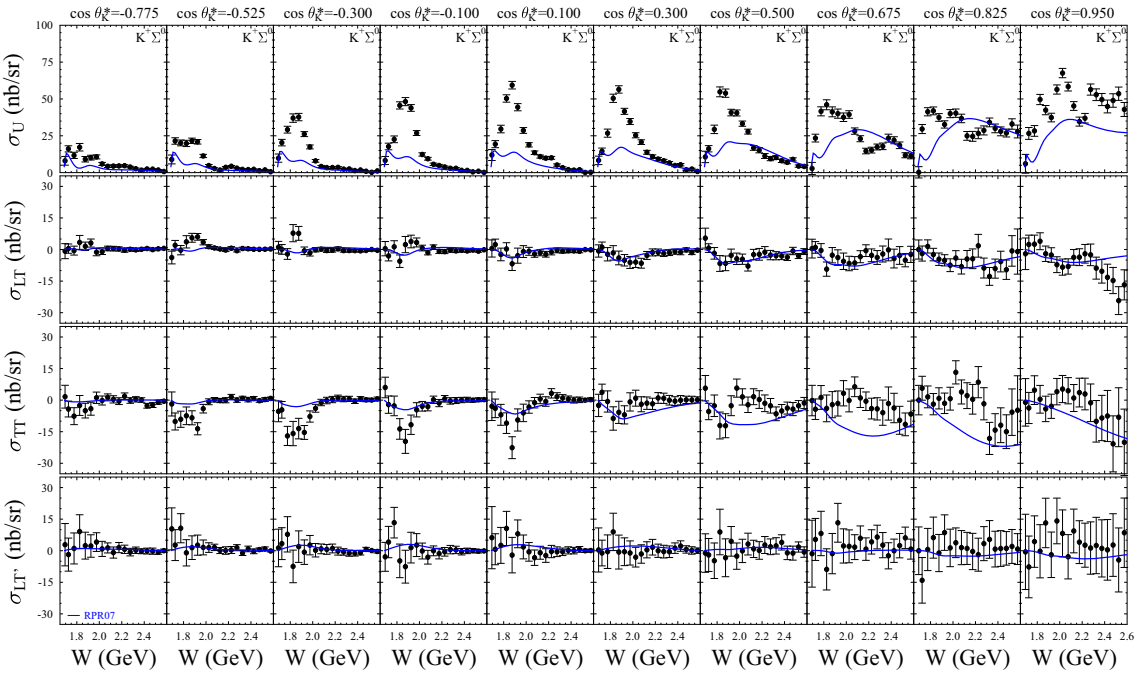

Fig. 6 Structure functions $\sigma_U = \sigma_T + \epsilon\sigma_L$, σ_{LT}, σ_{TT}, and $\sigma_{LT'}$ (nb/sr) from CLAS data for $K^+\Sigma^0$ production versus W (GeV) for E_{beam}=5.5 GeV for Q^2=1.80 GeV^2 and $\cos\theta^*_K$ values as shown [43]. The error bars represent the statistical uncertainties only. The blue curves are from the hybrid RPR-2007 KY model from Ghent [48]

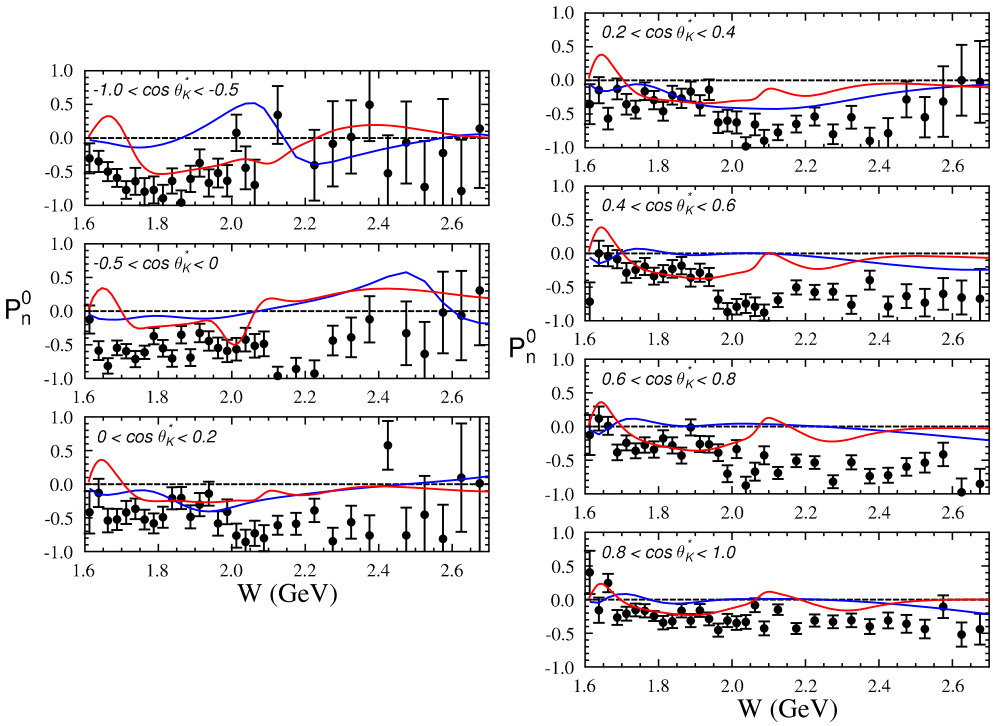

Fig. 7 Induced polarization of the final state hyperon in the reaction $ep \rightarrow e'K^+\Lambda$ from CLAS data at an average Q^2=1.9 GeV^2 for E_{beam}=5.5 GeV and $\cos\theta^*_K$ ranges as shown [44]. The error bars represent the statistical uncertainties only. The red curves are from the isobar model of Maxwell [47] and the blue curves are from the hybrid RPR-2011 KY model from Ghent [49]

(blue curves). Both the MX and RPR models include all well-established N^* states in the PDG listings with spins $J \leq \frac{5}{2}$. The MX model incorporates the u-channel Y^* states ($\Lambda(1405)\frac{1}{2}^-$, $\Lambda(1670)\frac{1}{2}^-$, $\Lambda(1820)\frac{1}{2}^+$, $\Lambda(1880)\frac{3}{2}^+$, $\Sigma(1385)\frac{3}{2}^+$, $\Sigma(1775)\frac{5}{2}^-$, $\Sigma(1915)\frac{5}{2}^+$, $\Sigma(1940)\frac{3}{2}^-$) along with the t-channel $K^*(892)$ and $K_1(1270)$ exchanges. The RPR model does not include any u-channel contributions, but does include the exchange of the K and K^* kaonic trajectories. Both the MX and RPR models were developed based on fits to the extensive and precise photoproduction data from CLAS and elsewhere, and describe those data reasonably well. However, they utterly fail to describe the electroproduction data in any of the kinematic phase space.

Reliable information on KY hadronic decays from N^*s is not yet available due to the lack of an adequate reaction model. However, after such a model is developed, the N^* electrocoupling amplitudes for states that couple to KY can be obtained from fits to the extensive existing CLAS KY electroproduction data over the range $0.5 < Q^2 < 4.5$ GeV^2, which should be carried out independently in different bins of Q^2 with the same KY hadronic decays, extending the available information on these N^* states. The development of reaction models for the extraction of the $\gamma_v NN^*$ electrocouplings from the KY electroproduction channels is urgently needed. It is important to note that the statistical quality of the KY data from the existing CLAS measurements is comparable to that of the CLAS $\pi\pi N$ data from which the electrocouplings of many N^* states have already successfully been extracted.

Work is presently underway to further develop the existing single-channel Ghent RPR model [49] based on a combined refit of the γp and $\gamma^* p$ data from CLAS in the kinematic range W up to 2.6 GeV and Q^2 up to 4.5 GeV^2. These fits should include the N^* electrocoupling parameters and their associated uncertainties based on presently available extractions [29]. This work should also include an improved description of the non-resonant background contributions in the $K^+\Lambda$ and $K^+\Sigma^0$ final states. The comparison of the RPR model to the data significantly under-represents the reaction strength of the data as seen most clearly in the unpolarized cross sections σ_U for the $K^+\Lambda$ and $K^+\Sigma^0$ channels in Figs. 5 and 6. This model development will then set the stage for further extension of this model into the kinematic range relevant for the planned studies with CLAS12 in kinematics with W up to 3 GeV and Q^2 up to 12 GeV^2. Ultimately, however, these electroproduction data need to be confronted within a global multi-channel model. Such efforts are getting underway by the ANL-Osaka [50], Bonn-Gatchina [51], and JPAC at JLab [52] groups.

It is also important to note that the πN and $\pi\pi N$ electroproduction channels represent the two dominant exclusive channels in the resonance region. The knowledge of the electroproduction mechanisms for these channels is critically important for N^* studies in channels with smaller cross sections such as $K^+\Lambda$ and $K^+\Sigma^0$ production, as they can be significantly affected in leading order by coupled-channel effects produced by their hadronic interactions in the pionic channels. Ultimately, such effects need to be properly included in the KY reaction models.

3 CLAS12 N^* Program

As part of the upgrade of the JLab accelerator from a maximum electron beam energy of 6 GeV to a maximum energy of 12 GeV, a new large acceptance spectrometer called CLAS12 was designed for experimental Hall B to replace the CLAS spectrometer. The new CLAS12 spectrometer [53] was designed for operation at beam energies up to 11 GeV (the maximum possible for delivery to Hall B) and will operate at a nominal beam-target luminosity of 1×10^{35} cm^{-2} s^{-1}, an order of magnitude increase over previous CLAS operation. This luminosity will allow for precision measurements of cross sections and polarization observables for many exclusive reaction channels for invariant energy W up to 3 GeV, the full decay particle phase space, and four momentum transfer Q^2 up to 12 GeV^2. The full physics program for CLAS12 has focuses on measurements of the spatial and angular momentum structure of the nucleon, investigation of quark confinement and hadron excitations, and studies of the strong interaction in nuclei. The commissioning of the new CLAS12 spectrometer is scheduled to take place in the winter of 2017/2018, followed in the spring of 2018 by the first physics running period.

CLAS12, like it predecessor CLAS, is a large acceptance spectrometer designed to cover a large angular phase space for the electroproduction of exclusive final states. At the heart of CLAS12 is a pair of newly constructed superconducting magnet systems. A six-fold symmetric torus magnet about the beamline is used for momentum analysis for forward-going charged particles. Charged particle tracking in the polar angle range from $5^\circ \rightarrow 35^\circ$ is accomplished using three layers of drift chambers in each 60°-wide sector between the coils with tracking layers before, within, and after the torus field. Downstream of the torus and drift chambers are a set of Cherenkov counters for hadron identification, time-of-flight scintillators for precise timing measurements, and electromagnetic calorimeters to identify electrons and neutral particles. Just upstream of the torus in the angular range from $2.5^\circ \rightarrow 4.5^\circ$ is a forward tagging system for measuring the electrons associated with quasi-real photoproduction in the range of $Q^2 < 0.2$ GeV^2.

A 5-T superconducting solenoid is used for momentum analysis for the central region of CLAS12 ($35^\circ \rightarrow 125^\circ$), while also serving as the magnetic shield to sweep away the dominant low-energy Møller background produced in the beam-target interactions. Within the solenoid is located a central tracking system for charged particles based on a combined silicon strip and micromegas tracker, a time-of-flight scintillator system for precision timing, and a scintillator-based neutron detector. Located between the forward and central CLAS12 detectors is a large-area Cherenkov counter for identification of electrons as part of the primary readout trigger.

The N^* program with CLAS12 consists of three approved experiments. E12-09-003 [54] will focus on the non-strange final states (primarily πN, ηN, $\pi\pi N$) with an 11 GeV beam and E12-06-108A [55] and E12-16-010A [56] will focus on the strange final states (primarily $K^+\Lambda$ and $K^+\Sigma^0$) with beam energies of 6.6, 8.8, and 11 GeV. These experiments will allow for the determination of the Q^2 evolution of the electrocoupling parameters for N^* states with masses in the range up to 3 GeV in the regime of Q^2 up to 12 GeV^2 and will be part of the first production physics running period with CLAS12 in 2018. The experiments will collect data simultaneously using a longitudinally polarized 11 GeV electron beam on an unpolarized liquid-hydrogen target.

The program of N^* studies with the CLAS12 detector has a number of important primary objectives. These include:

(i) To study the higher-lying states in the N^* spectrum for $W > 1.8$ GeV where spectroscopy information is limited and for which both constituent quark models [8,9] and LQCD calculations [10] show is populated with a myriad of states. In particular, the data from KY electroproduction experiments will provide for important precision tests to confirm signals of new baryon states observed based on KY photoproduction data [34].

(ii) The extraction of electrocoupling amplitudes as a function of Q^2 for N^* states of different quantum numbers over the full nucleon resonance region is essential to understand the regime where the external meson–baryon cloud transitions to dynamics dominated by confined quarks and gluons. These data can

be used to check theoretical expectations for the meson–baryon cloud generation from the confinement regime. Improved understanding of the affects of the meson–baryon cloud and its affect on understanding N^* structure was a critical step towards resolving the 50-year puzzle surrounding the $N^*(1440)1/2^-$ Roper resonance [57].

(iii) To access diquark correlations in N^* structure. These configurations of non-point-like diquarks are an important part of N^* structure and the $\gamma_v NN^*$ transition amplitudes that are determined by the dressed quark mass function through dynamical chiral symmetry breaking [7]. The contributions depend on the quantum numbers of the N^* states. They are expected to be maximal for $Q^2 < 5$ GeV^2, and maximal sensitivity is expected in the range of Q^2 from 2 to 5 GeV^2 where contributions from meson–baryon cloud effects are substantially reduced.

(iv) To map out the quark structure of the dominant N^* states from the acquired electroproduction data through the exclusive final states including the non-strange channels $\pi^0 p$, $\pi^+ n$, ηp, $\pi^+\pi^- p$, as well as the dominant strangeness channels $K^+\Lambda$ and $K^+\Sigma^0$. This objective is motivated by results from existing analyses such as those shown in Fig. 3, where it is seen that the meson–baryon dressing contribution to the N^* structure decreases rapidly with increasing Q^2. The data can be described approximately in terms of dressed quarks already for Q^2 up to 3 GeV^2. It is therefore expected that the data at $Q^2 > 5$ GeV^2 can be used more directly to probe the quark substructure of the N^* states [7]. The comparison of the extracted resonance electrocoupling parameters from this new higher Q^2 regime to the predictions from LQCD and DSE calculations will allow for a much improved understanding of how the internal dressed quark core emerges from QCD and how the dynamics of the strong interaction are responsible for the formation of N^* states of different quantum numbers.

(v) To investigate the dynamics of dressed quark interactions and how they emerge from QCD to generate N^* states of different quantum numbers. This work is motivated by recent advances in the DSE approach [58, 59] and LQCD [60], which have provided links between the dressed quark propagator, the dressed quark scattering amplitudes, and the QCD Lagrangian. These approaches also relate the momentum dependence of the dressed quark mass function to the $\gamma_v NN^*$ electrocouplings for N^* states of different quantum numbers. While the available electroproduction data from CLAS at 6 GeV beam energy provides only a glimpse of the evolution of the running quark mass function, future results on resonance electrocouplings from CLAS12 at beam energies up to 11 GeV will expand the kinematic range up to $Q^2 \leq 12$ GeV^2 [54–56]. These data will then allow for an exploration of the dressed quark mass function to distance scales where the transition from strong to perturbative QCD occurs. DSE analyses of the extracted N^* electrocoupling parameters have the potential to allow for investigation of the origin of quark-gluon confinement in baryons and the nature of more than 98% of the hadron mass generated non-perturbatively through DCSB, since both of these phenomena are rigorously incorporated into the DSE approach [7]. Efforts are being made to study the sensitivity of the proposed electromagnetic amplitude measurements to different parameterizations of the momentum dependence of the quark mass [61].

(vi) To offer constraints from resonance electrocoupling amplitudes on the Generalized Parton Distributions (GPDs) describing $N \rightarrow N^*$ transitions. We note that a key aspect of the CLAS12 measurement program is the characterization of exclusive reactions at high Q^2 in terms of GPDs. The elastic and $\gamma_v NN^*$ transition form factors represent the first moments of the GPDs [62,63], and they provide for unique constraints on the structure of nucleons and their excited states. Thus the N^* program at high Q^2 represents the initial step in a reliable parameterization of the transition $N \rightarrow N^*$ GPDs and is an important part of the larger overall CLAS12 program studying exclusive reactions.

4 Concluding Remarks

The study of the spectrum and structure of the excited nucleon states represents one of the foundations for the measurement program in Hall B with the CLAS spectrometer. To date, measurements with CLAS have provided a dominant amount of precision data (cross sections and polarization observables) for a number of different exclusive final states for Q^2 from 0 to 4.5 GeV^2 for W up to 2.5 GeV and the full center-of-mass angular range of the final state decay products. From the πN, ηN, and $\pi\pi N$ data, the electrocouplings of most N^* states up to ~1.8 GeV have been extracted for the first time. A powerful cross-check of these findings is the good agreement of the extracted N^* electrocouplings from independent analyses of different final states. With the development and refinement of reaction models to describe the extensive CLAS $K^+\Lambda$ and $K^+\Sigma^0$ electroproduction data, the CLAS data from the strangeness channels is expected to provide an

important complement to study the electrocoupling parameters for higher-lying N^* resonances with masses above 1.6 GeV and will serve as an important cross-check of the extracted electrocouplings from the $\pi\pi N$ channel.

The N^* program with the new CLAS12 spectrometer will extend these studies up to Q^2 of 12 GeV^2, the highest photon virtualities ever probed in exclusive reactions. This program will ultimately focus on the extraction of the $\gamma_v NN^*$ electrocoupling amplitudes for the s-channel resonances that couple strongly to the non-strange final states πN, ηN, and $\pi\pi N$, as well as the strange $K^+\Lambda$ and $K^+\Sigma^0$ final states. These studies in concert with theoretical developments will allow for insight into the strong interaction dynamics of dressed quarks and their confinement in baryons over a broad Q^2 range. The data will address the most challenging and open problems of the Standard Model on the nature of hadron mass, quark-gluon confinement, and the emergence of the N^* states of different quantum numbers from QCD.

Acknowledgements This work was supported by the U.S. Department of Energy, Office of Science, Office of Nuclear Physics under contract DE-AC05-06OR23177. The author is grateful for many lengthy and fruitful discussions on this topic with Victor Mokeev and Ralf Gothe. The author also thanks the organizers of the N^*2017 Workshop for the opportunity to present this work and participate in this workshop.

References

1. The 2015 Long Range Plan for Nuclear Science, https://science.energy.gov/~/media/np/nsac/pdf/2015LRP/2015_LRPNS_091815.pdf. Accessed 23 Aug 2017
2. I.G. Aznauryan, V.D. Burkert, Prog. Part. Nucl. Phys. **67**, 1 (2012)
3. J. Segovia et al., Phys. Rev. Lett. **115**, 171801 (2015)
4. I.C. Cloët, C.D. Roberts, Prog. Part. Nucl. Phys. **77**, 1 (2014)
5. I.V. Anikin et al., Phys. Rev. D **92**, 014018 (2015)
6. H. Kamano, S.X. Nakamura, T.-S.H. Lee, T. Sato, Phys. Rev. C **88**, 035201 (2013)
7. I.G. Aznauryan et al., Int. J. Mod. Phys. E **22**, 1330015 (2013)
8. S. Capstick, N. Isgur, Phys. Rev. D **34**, 2809 (1986)
9. U. Löring, BCh. Metsch, H.R. Petry, Eur. Phys. J. A **10**, 395 (2001)
10. J.J. Dudek, R.G. Edwards, Phys. Rev. D **85**, 054016 (2012)
11. B.A. Mecking et al., Nucl. Inst. Methods A **503**, 513 (2003)
12. E. Isupov et al., CLAS Collaboration, Phys. Rev. C **96**, 025209 (2017)
13. CLAS Physics Database, CLAS physics database, http://clasweb.jlab.org/physicsdb. Accessed 23 Aug 2017
14. I. Aznauryan et al., Phys. Rev. C **80**, 055203 (2009)
15. K. Park et al., CLAS Collaboration, Phys. Rev. C **91**, 045203 (2015)
16. M. Ripani et al., CLAS Collaboration, Phys. Rev. Lett. **91**, 022002 (2003)
17. G.V. Fedotov et al., CLAS Collaboration, Phys. Rev. C **79**, 014204 (2009)
18. V.I. Mokeev, I.G. Aznauryan, Int. J. Mod. Phys. Conf. Ser. **26**, 1460080 (2014)
19. V.I. Mokeev et al., Phys. Rev. C **93**, 025206 (2016)
20. V.I. Mokeev, The 11th International Workshop on the Physics of Excited Nucleons-N*2017, (2017)
21. J.J. Kelly et al., Phys. Rev. C **75**, 025201 (2007)
22. A.N. Villano et al., Phys. Rev. C **80**, 035203 (2009)
23. V.V. Frolov et al., Phys. Rev. Lett. **282**, 45 (1999)
24. N.F. Sparveris et al., Phys. Rev. Lett. **94**, 022203 (2005)
25. I.G. Aznauryan, V.D. Burkert, Phys. Rev. C **85**, 055202 (2012)
26. V.I. Mokeev, Few Body Syst. **57**, 909 (2016)
27. E. Santopinto, M.M. Giannini, Phys. Rev. C **86**, 065202 (2012)
28. B. Julia-Diaz et al., Phys. Rev. C **77**, 045205 (2008)
29. Nucleon Resonance Photo-/Electrocouplings Determined from Analyses of Experimental Data on Exclusive Meson Electroproduction off Protons https://userweb.jlab.org/~mokeev/resonance_electrocouplings/. Accessed 23 Aug 2017
30. D.S. Carman, Few. Body Syst. **57**, 941 (2016)
31. J. Beringer et al., PDG. Phys. Rev. D **86**, 010001 (2012)
32. A.V. Sarantsev et al., Eur. Phys. J. A **25**, 441 (2005)
33. V. Shklyar, H. Lenske, U. Mosel, Phys. Rev. C **72**, 015210 (2005)
34. A.V. Anisovich, R. Beck, E. Klempt, V.A. Nikonov, A.V. Sarantsev, U. Thoma, Eur. Phys. J. A **48**, 15 (2012)
35. C. Patrignani et al., Particle Data Group, Chin. Phys. C **40**, 100001–10 (2016)
36. M.E. McCracken et al., CLAS Collaboration, Phys. Rev. C **81**, 025201 (2010)
37. B. Dey et al., CLAS Collaboration, Phys. Rev. C **82**, 025202 (2010)
38. See PDG listings at: http://pdg.lbl.gov/2017/reviews/rpp2017-rev-n-delta-resonances.pdf. Accessed 23 Aug 2017
39. V.D. Burkert, Proceedings of 22nd International Symposium on Spin Physics (SPIN 2016), arXiv:1702.07072
40. B.A. Raue, D.S. Carman, Phys. Rev. C **71**, 065209 (2005)
41. P. Ambrozewicz et al., CLAS Collaboration, Phys. Rev. C **75**, 045203 (2007)
42. R. Nasseripour et al., CLAS Collaboration, Phys. Rev. C **77**, 065208 (2008)
43. D.S. Carman et al., CLAS Collaboration, Phys. Rev. C **87**, 025204 (2013)

44. M. Gabrielyan et al., CLAS Collaboration, Phys. Rev. C **90**, 035202 (2014)
45. D.S. Carman et al., CLAS Collaboration, Phys. Rev. Lett. **90**, 131804 (2003)
46. D.S. Carman et al., CLAS Collaboration, Phys. Rev. C **79**, 065205 (2009)
47. O. Maxwell, Phys. Rev. C **85**, 034611 (2012)
48. T. Corthals et al., Phys. Lett. B **656**, 186 (2007)
49. L. De Cruz et al., Phys. Rev. C **86**, 015212 (2012)
50. H. Kamano, JPS Conf. Proc. **13**, 010012 (2017)
51. A. Sarantsev, ECT* Workshop, Nucleon Resonances: From Photoproduction to High Photon Virtualities, Oct. 12–16, 2015, Trento, Italy http://boson.physics.sc.edu/~gothe/ect*-15/intro.html. Accessed 23 Aug 2017
52. JLab Joint Physics Analysis Center, https://jpac.jlab.org. Accessed 23 Aug 2017
53. See CLAS12 webpage at http://www.jlab.org/Hall-B/clas12-web. Accessed 23 Aug 2017
54. V.D. Burkert, P. Cole, R. Gothe, K. Joo, V. Mokeev, P. Stoler, Nucleon Resonance Studies with CLAS12, JLab Experiment E12-09-003
55. D.S. Carman, R. Gothe, V. Mokeev, Exclusive $N^* \to KY$ Studies with CLAS12, JLab Experiment E12-06-108A
56. D.S. Carman, R. Gothe, V. Mokeev, Nucleon Resonance Structure Studies Via Exclusive KY Electroproduction at 6.6 GeV and 8.8 GeV, JLab Experiment E12-16-010A
57. V.D. Burkert, C.D. Roberts, arXiv:1710.02549 (2017)
58. C.D. Roberts, J. Phys. Conf. Ser. **630**, 012051 (2015)
59. J. Segovia et al., Few Body Syst. **55**, 1185 (2015)
60. R.G. Edwards, J.J. Dudek, D.G. Richards, S.J. Wallace, AIP Conf. Proc. **1432**, 33 (2012)
61. I.C. Clöet, C.D. Roberts, A.W. Thomas, Phys. Rev. Lett. **111**, 101803 (2013)
62. L.L. Frankfurt et al., Phys. Rev. Lett. **84**, 2589 (2000)
63. K. Goeke, M.V. Polyakov, M. Vanderhaeghen, Prog. Part. Nucl. Phys. **47**, 401 (2001)